RESEARCH ARTICLE

National Science Open
5: 20250078, 2026
https://doi.org/10.1360/nso/20250078

Materials Science

Special Topic: Intelligent Materials and Devices

A high-accuracy Braille recognizing sensing device bio-inspired by human touch sensation based on microstructure-based sensor and machine learning method

Lihong Wang[1,#], Zhou Zhang[1,#], Xindi An[1], Jiaxu Liu[2], Lijun Qu[2], Junyang Li[1,*], Mingwei Tian[2,*] & Qi Wen[1,*]

[1]*Shandong Key Laboratory of Intelligent Sensing Chip and System, Department of Electronic Engineering, Ocean University of China, Qingdao 266400, China;*
[2]*Research Center for Intelligent & Wearable Technology, College of Textiles & Clothing, Collaborative Innovation Center for Eco-Textiles of Shandong Province, Qingdao University, Qingdao 266071, China*

#Contributed equally to this work.
*Corresponding authors (emails: lijunyang@ouc.edu.cn (Junyang Li); mwtian@qdu.edu.cn (Mingwei Tian); wenqi@ouc.edu.cn (Qi Wen))

Received 21 November 2025; Revised 8 December 2025; Accepted 11 December 2025; Published online 12 December 2025

Abstract: Braille learning is essential to communicate and work for visually impaired people (VI). However, a convenient and portable Braille learning device has not been investigated. Herein, a convenient and high-accuracy Braille learning-enabled tactile sensing system is developed to help VI learning Braille themselves. The tactile sensing system based on tailored micropatterned tactile sensor through sliding mode on Braille, which is bio-inspired by human touching sensation. It achieved a high recognition accuracy of 98.96% for 26 English letters for Braille. The tactile sensor with a tiny size (3 mm×3 mm×2 mm) exhibited a high sensitivity of 0.11 kPa^{-1}, which is based on two micro-dome structures with the same dimension as the dot on Braille. The tactile sensing device is fabricated by the tailored sensor, process circuit and microprogrammed control unit to recognize Braille; the sensing device can help VI learning and writing Braille. This work presents a practical theory for VI learning Braille themselves.

Keywords: Braille learning, bio-inspired, high-accuracy recognition, micro-dome pressure sensor

INTRODUCTION

Braille is an essential way for the visually impaired people (VI), such as the blind people, to perceive and communicate with the world [1,2]. Braille is a kind of six-dot system that consists of three rows and two columns of raised dots, and different combinations of raised dots are used to represent different characters [3–5]. People read and learn Braille through touching. However, learning Braille is always from teachers, which is still a challenge for most VI because of its high cost, time-consuming and laborious [6,7]. In recent years, wearable Braille recognition devices have been developed to assist the VI in reading and communicating. Therefore, developing a high-accuracy and portable Braille recognition system is important for the VI.

Advances in flexible electronic devices and artificial intelligence (AI) have enabled new directions to

realize efficient and real-time Braille recognition [8–10]. There are some works reporting the AI-based Braille recognition with flexible tactile sensors [1,3]. For example, Qiao *et al*. [11] combined a nanomesh-reinforced graphene pressure sensor with a convolutional neural network (CNN), which can distinguish convex Braille numbers with an accuracy of 88%. High-performance flexible tactile sensor is one crucial component for collecting accurate Braille touching signals in the Braille recognition system. The ideal flexible tactile sensors require high sensitivity, fast response time, low hysteresis, excellent stability and long-term cycle durability [12–14]. Endowing microstructure such as micro-porous [15,16], micro-pyramid [17,18], micro-pillar [19,20] and micro-dome [21,22] to flexible materials is of great significance for the development of flexible tactile sensors. Also, the micropatterned polymer integrated with sensing active layer (such as graphene, MXene and multi-walled carbon nanotubes) can be widely used in four transduction mechanisms including piezoelectric [23], triboelectric [24], piezoresistive [25,26], and capacitive [27,28] flexible tactile sensors. Flexible micropatterned piezoresistive tactile sensors have been widely used because of high sensing performance, simple device configuration and fabrication process [25,26,29,30]. Besides, advanced neural network technology of AI is the other important role of the Braille recognition; machine learning algorithms such as support vector machine [31], CNN [32], and rapid situation learning [33] have been utilized to boost data identification, which can recognize Braille through receiving and learning digital sensing signals of the tactile sensors. However, most Braille recognition systems are still complex, non-portable and with a low accuracy.

In this paper, we develop a Braille recognition system based on a tailored piezoresistive flexible micro-dome sensor and a high-efficient AI method. The proposed micro-dome sensor exhibited an efficient and stable sensing performance, and output accurate sensing signals when touching Braille, which could enhance the Braille recognition accuracy through the arithmetic process of a one-dimensional (1D) CNN. Therefore, the micro-dome tactile sensor combined with a process circuit and microprogrammed control unit obtains sensing signals regarding finger touch, achieving Braille recognition of twenty-six letters, with a maximum recognition accuracy of 98.96%. The proposed Braille recognition system will be favorable for the visually impaired people learning, reading and writing Braille by themselves.

RESULTS AND DISCUSSION

Overall design and working mechanism of the tactile sensor

People recognize Braille mainly through touching. To help the VI learning Braille, many pressure sensors were developed for transmitting the touching signals to electrical signals. Traditional tactile sensors recognized Braille through pressing on the Braille such as one-channel flexible sensors and six-channel sensors. As shown in Figure 1, the one-channel flexible sensors output confused sensing signals and recognize Braille through a complex machine learning method. Then the six-channel sensor is hard for both normal people and VI to press on the Braille point by point correctly. Therefore, we designed a two-channel tactile sensor bio-inspired by human touch sensation, which recognizes Braille through sliding and touching. The two-channel sensor can be used more easily than the other two kinds of tactile sensors, and generates clear sensing signals to improve recognition accuracy.

We developed a tailored tactile finger-tip sensor for the VI learning Braille, which is bio-inspired by human

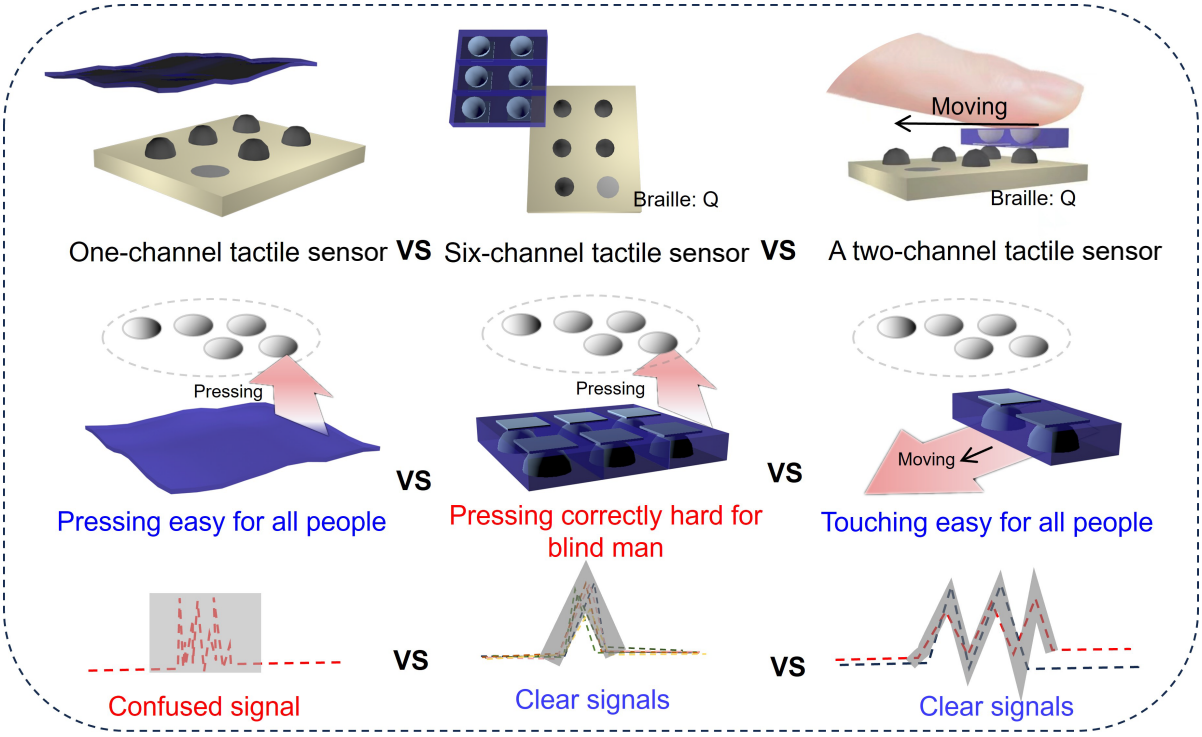

Figure 1 Comparison of one-channel, six-channel and two-channel flexible tactile sensors.

touching and moving on Braille, as shown in Figure 2a. The developed tactile sensor can touch the Braille through the fingertip, moving on the dots on Braille easily, which can also generate both stable and clear sensing signals. The sensing paths of the tactile sensor based on the two electrodes (2B-sensor) on the bottom layer are shown in Figure 2b, leading to sensing signals from the 2B-sensor when moving on the dots of Braille. The dots of Braille turn into pressure to the 2B-sensor; therefore, the 2B-sensor generated two paths of resistance variations in the process of recognizing Braille. Then, the sensing signal qualities are evaluated by a machine learning method shown in Figure 2c. The Braille sensing signals of 2B-sensor exhibited a higher recognition accuracy of 98.96% than flexible one-channel sensors [11,34,35], and image recognition [36] to recognize Braille in Figure 2d.

Microstructures can be utilized for increasing the sensing performance of pressure sensor, which has been proven in many previous works. The tailored tactile sensor we designed for Braille recognition was based on two microstructures with the same dimension as the dot on Braille (diameter is 1 mm) as shown in Figure 3a, the detail size for designing the sensor was shown in the side-view of the sensor on the Braille. Then in order to better understand the sensing mechanism of the designed tactile sensor, we theoretically explained the rationality regarding superior performance for the fabricated 2B-sensor as shown in the right side of Figure 3a, the microscopic view, finite element molding, equivalent-circuit diagram based on the contact area changing between the top and bottom' layer under different pressures. The 2B-sensors we developed generate deformation and resistance variation based on increased contact area between the top and bottom electronic layer under pressure, at the initial state, the top and bottom layer did not contact, the initial resistance of two sensing channels were R_1 and R_2 as shown in the schematic and equivalent-circuit diagram

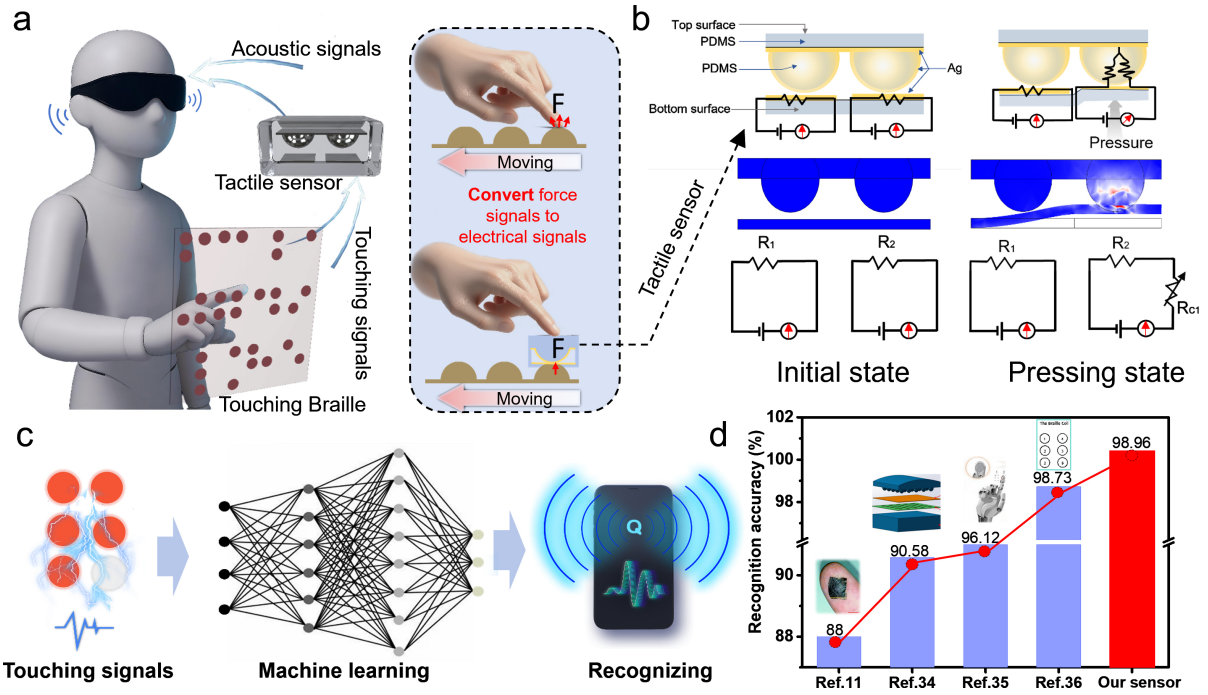

Figure 2 Demonstration of tailored micro-dome tactile sensors for recognizing Braille. (a) Schematic of the visually impaired person touching and learning Braille with a tactile sensor inspired by human finger moving on the dots of the Braille. (b) Schematics showing the resistance composition of the tactile sensor before and after pressure. (c) Schematic of Braille recognition process through a machine learning method. (d) Comparison of the Braille recognition accuracy through a machine learning method based on this work and previous report works.

of the 2B-sensor; after one channel of 2B-senor under pressure, one side of the micro-dome contact with the bottom electrode and generates deformation and resistance variation, the generated contact resistance in series with R_2 leading an increasing resistance in the R_2-channel; and when two channel of 2B-sensor under pressure, two side of the micro-dome contact with the bottom electrodes and generate deformation and resistance variation, the generated contact resistance in series with R_1 and R_2 leading an increasing resistance in both the R_1-channel and R_2-channel. The tailored 2B-sensor is specialized used to recognizing Braille, there are only the above three kinds of stress situations.

In Figure 3b, we analyzed the deformation and the local stress distribution of different microstructures through ANSYS, including no microstructure, micro-column, micro-pyramid and micro-dome. The substrate is polydimethylsiloxane (PDMS) film, the distance from the bottom layer to the top layer of four kinds of sensors are all 0.2 mm, three kinds of microstructures have the same length (1 mm) and height (0.5 mm). After pressing 0.35 mm on three kinds of sensors, the stress distribution of the sensor without microstructure concentrate on the outside, which will lead to the confused sensing signals of sensing dots on Braille; the stress distribution area of micro-column sensor concentrate on the bottom layer are bigger than the other two sensors, the extra stress distribution will also lead to the confused sensing signals because two dots on Braille are close in distance. Therefore, the micro-pyramid sensor and micro-dome sensor are more suitable for sensing Braille, and the deformation of micro-dome sensor is larger than the micro-pyramid sensor, larger deformation will occur at the contact spots, which leading the larger resistance variation of

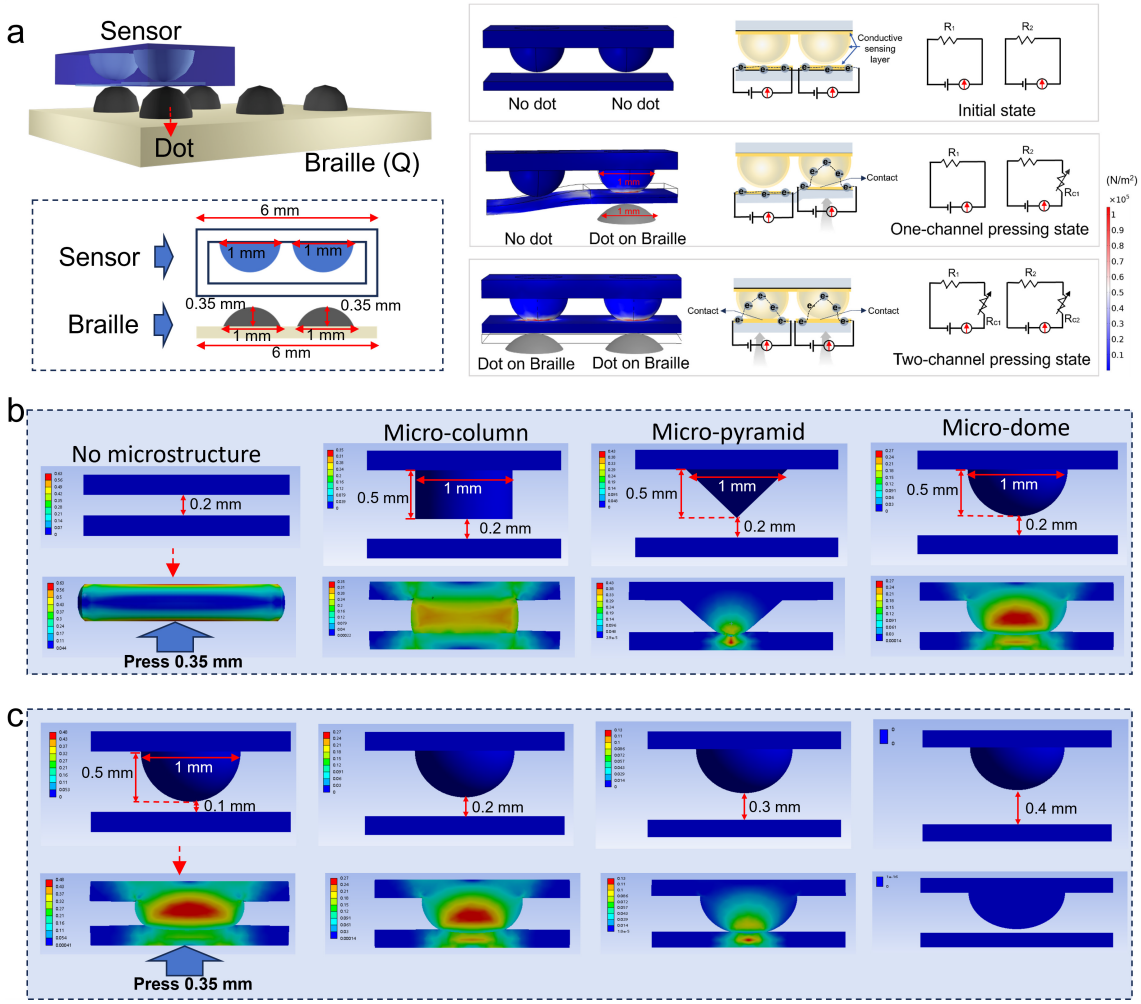

Figure 3 Structure design and analysis of tactile sensor. (a) Illustration of the dimensions of the tactile sensor and scanned Braille, and finite-element calculations show the deformation and the local stress distribution of tactile sensor when without dot on Braille, with one-side dot, and with two-side dots on Braille. (b) Finite-element calculations show the deformation and the local stress distribution of tactile sensor with no microstructure, micro-column, micro-pyramid, and micro-sphere. (c) Finite-element calculations show the deformation and the local stress distribution of micro-sphere tactile sensor with different distances.

piezoresistive sensor under pressure. In conclusion, micro-dome structure was chosen to form tactile sensor for sensing Braille accurately.

At last, the height of dots on Braille is 0.35 mm, the distance from the bottom layer and top layer is another factor which influence the sensing performance of tactile sensor, as shown in Figure 3c, we analyzed the deformation and the local stress distribution of micro-dome sensor with the distance of 0.1, 0.2, 0.3 and 0.4 mm (from top of micro-dome to bottom layer) at a 0.35 mm distance pressure through ANSYS, the shorter distance lead to the stress distribution concentrate on the bottom layer, which lead to the confused sensing signals because two dots on Braille are close in distance; the longer distance lead to a small or little deformation which exhibited poor sensing performance; therefore, the micro-dome sensor with 0.2 mm distance we choose for sensing Braille, which exhibited both proper stress distribution concentrate on the bottom layer than sensor with 0.1 mm, and exhibited larger deformation than sensor with the distance of 0.3

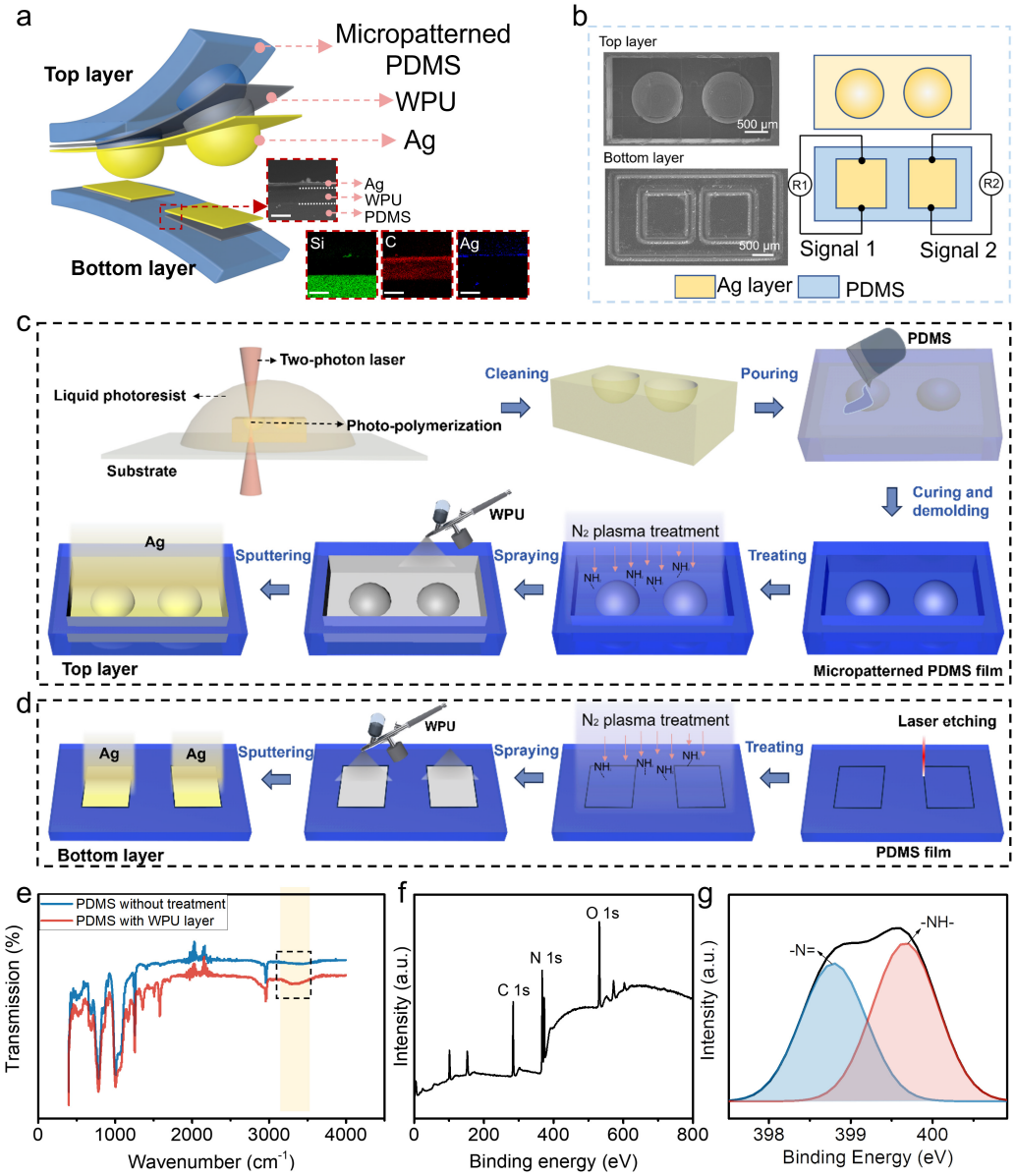

Figure 4 Characterization of the tactile sensor. (a) Explosive view of the micro-sphere tactile sensor (scale bar is 5 μm). (b) Scanning electron microscopy (SEM) images of the top and bottom layers of the 2B-sensor in top view, with right side showing the schematic of the top and bottom layers 2B-sensor. (c, d) Fabrication procedures of the top and bottom layers of the sensor. (e) FTIR spectra of the PDMS film before and after N_2-plasma treatment. (f, g) XPS survey spectra of spectrum N 1s region of N_2 plasma-treated PDMS film.

and 0.4 mm.

Fabrication and morphology of tactile sensor

The two-channel micro-dome tactile sensor (2B-sensor) is composed of two layers including the micro-dome top layer and the flat bottom layer, shown in Figure 4a, b. The top layer is composed of micro-dome PDMS film, waterborne polyurethane (WPU) film and Ag layer; the bottom layer is composed of flat PDMS film, a

WPU film and Ag electrodes. The distribution of Ag layer on the micro-dome and flat PDMS film could be observed, then the surface morphology of the bottom layer was observed by scanning electron microscopy (SEM) and energy dispersive X-ray spectroscopy (EDS) mapping, in which Ag layer is overlaid on the PU layer adhered on the PDMS film, which clearly revealed the distribution of Si (from PDMS), C (from WPU) and Ag elements, respectively. The top-view SEM images of the top and bottom 2B-sensor were shown in Figure 4b. Figure 4c, d illustrated the fabrication process of the 2B-sensor, the top micro-dome PDMS film was peeling off from a two-photon laser writing micro-dome mold, and then WPU solution was sprayed on the top micro-dome PDMS film after plasma treatment in N_2, followed by Ag layer coating on both sides of PDMS/WPU film to form top conductive micro-patterned PDMS/WPU/Ag substrate; the bottom flat PDMS/WPU/Ag film was first etched by laser to form two area, then plasma treated in N_2, spraying WPU solution, after curing in oven, at last the Ag layer was coated on the PDMS/WPU film to obtain two conductive electrodes (Detailed description is in the MATERIALS AND METHODS). Finally, the top and bottom films were assembled into the tactile sensor by top-bottom structure as shown in Figure S1. The WPU layer distributed and adhered to the PDMS stably because there is a local change in the material properties at the plasma-treated surface of PDMS film. The Fourier transform infrared (FTIR) spectra of PDMS film and PDMS film after N_2-plasma treatment with WPU layer are shown in Figure 4e, indicating that there is a local change in the material properties at the plasma-treated surface. Compared with un-treated PDMS, the stretching of OH give rise to a broad peak from 3500 to 3000 cm^{-1}, for the N 1s spectra of an N_2 plasma treatment PDMS in the X-ray photoelectron spectroscopy (Figure 4f, g), two peaks with binding energies 399.6 and 401.2 eV corresponding to amine group (–NH–) and amide group ($–NH_2$), which indicated the hydroxyl and amide group producing by N_2-Plasma treatment, thus, the treated PDMS can provide active sites for WPU layer [37]. Also, the hydroxy, amine group and amide group enhance the stability of the Ag layer adhering on the WPU/PDMS surface, which has been proven in our previous work [21].

Sensing performance of tactile sensor

The tailored micro-dome 2B-sensor we developed for Braille recognition was tiny, with a high and stable sensing performance. The tiny 2B-sensor on the finger-tip was shown in Figure 5a. Two micro-domes sensors with one electrode (1B-senor) and two electrodes (2B-sensor) were proposed and fabricated as shown in Figure 5b and Figure S2, then the sensitivities of 1B-sensor and 2B-sensor were measured by pressing one side micro-dome of the sensor, the sensitivity of 1B-sensor was a little higher than 2B-sensor in the 0–3 kPa pressure. Hysteresis is the relative difference in the area underneath the $\Delta R/R_0$ versus pressure curves under loading and unloading, which can be defined as the degree of hysteresis (DH). The equation for DH is as follows:

$$\mathrm{DH}(\%) = \frac{A_{\mathrm{Releasing}} - A_{\mathrm{Loading}}}{A_{\mathrm{Loading}}} \times 100\%, \tag{1}$$

where A_{Loading} and $A_{\mathrm{Releasing}}$ are the areas of the curves under loading and releasing, respectively. The 2B-sensor exhibited a low hysteresis. Figure 5c depicts the resistance variation of a 2 kPa loading-releasing cycle with a margin hysteresis of 14%. And to evaluate the stable sensing performance of 2B-sensor, a real-time pressure response of sensors with quickly loading low pressures (5, 10 and 15 Pa) and high pressures (1, 2 and 3 kPa) was investigated (Figure 5d, e). The results show that the 2B-sensor presented stable sensing

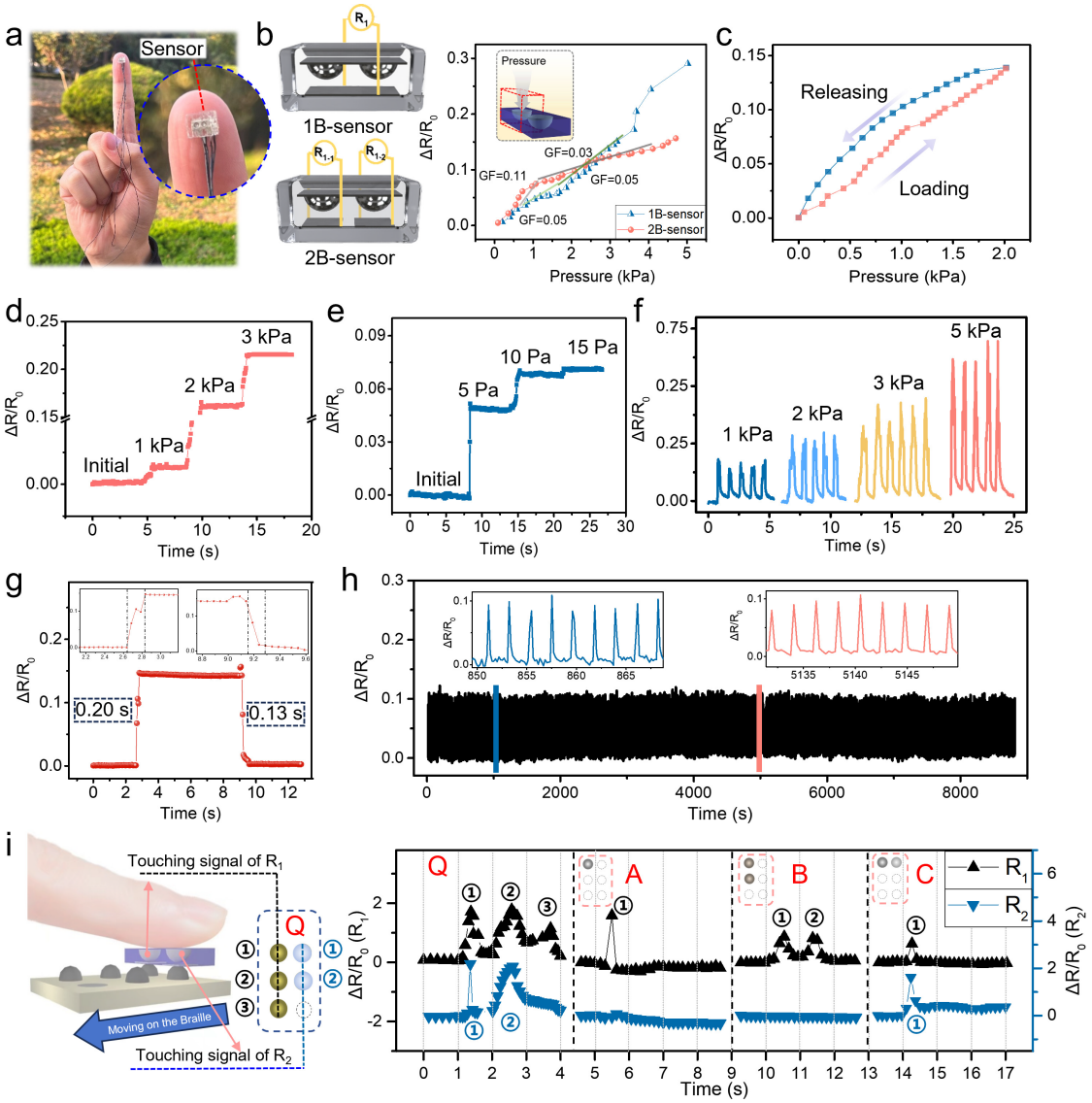

Figure 5 Pressure-sensing performance of micro-dome sensor. (a) Photograph of 2B-sensor on the fingertip. (b) Schematic of one-channel (1B-sensor) and two-channel tactile sensor (2B-sensor), and the relative resistance variations of 1B-sensor and 2B-sensor under different pressures. (c) Relative resistance variation of the 2B-sensor during a 2 kPa pressure loading-releasing cycle. (d) Relative resistance variation of 2B-sensor with increasing pressure (1, 2 and 3 kPa). (e) Relative resistance variation of 2B-sensor with increasing subtle pressure (5, 10 and 15 Pa). (f) Relative resistance variation under different loads. (g) Response time of 2B-sensor under pressure 2 kPa. (h) Piezoresistive repeatability of the 2B-sensor under repeated loading/unloading at a pressure of 2 kPa for 5000 cycles. (i) Tactile sensing process of 2B-sensor moving and recognizing Braille "Q", and tactile signals detected by the 2B-sensor when compressing the convex Braille letters Q, A, B and C.

performance with high sensitivity and range detection. Figure 5f shows the real-time response of the 2B-sensor for escalating loading/unloading pressure of 1, 2, 3 and 5 kPa with five cycles at each pressure. Then during the process of loading 2 kPa on 2B-sensor, the corresponding response time and recovery time was 0.2 and 0.13 s, respectively (Figure 5g). Under the load of 2 kPa of externally applied pressure, the relative resistance of sensor signals did not deteriorate significantly after 5000 pressure loading/releasing cycles in 8000 s in Figure 5h. The sensor exhibited a good sensitivity, response time, stability and durability, which is

proper for Braille recognition. Then the tester compressed convex Braille letters Q, A, B and C using the 2B-sensor, the typical tactile signals were illustrated in Figure 5i. The sensing meachism of 2B-sensor was the generated compression while moving on the Braille, the sensor transformed the compression into resistance variation, therefore, the different Braille can be distinguished by the digital sensing signals from wave forms. Also, the 2B-sensor exhibited a good sensing performance when undera high pressure and in water environment in Figure S3, indicating good durability and waterproof performance.

Application of tactile sensor recognizing and learning Braille

The Braille can help the VI reading, learning, writing and communicating with the world (Figure 6a); therefore, it is essential and meaningful for the VI learning Braille. A tailored Braille board for tactile sensor was designed as shown in Figure 6b. Then, tactile sensing signals of 2B-sensor and 1B-sensor touching on 26 English letters are shown in Figure 6c and Figure S4. We collected the data of tactile sensor sensing signals on Braille (26 English letters) through sequential touching Braille, and used algorithms to classify Braille. Here, we compared six kinds of machine learning methods as shown in Figure 6d. The CNN algorithm realizes the recognition accuracy with 98.96%, which is higher than the other algorithms. The AI method of CNN was utilized to boost Braille sensing data identification in Figure 6e. CNN is an efficient algorithm to realize the information mining and automatic classification when combined with a developed tactile sensor, which contains three 1D convolutional layers and three fully connected layers, and 1D CNN has a smaller network size and computational load. The databases for training and testing CNN are generated through sequential touching Braille, and the data in the databases is the resistance variation of tactile sensor during the sequential touching process. It was observed that the precise recognition of 2B-sensor is 98.96%, which is higher than 1B-sensor (75.66%) (Figure 6f, Figures S5 and S6). Also, the recognition accuracy of 2B-sensor is higher than most proposed tactile sensors for recognizing Braille.

In the process of learning and writing Braille, the tactile side of the Braille is the opposite side of writing Braille, shown in Figure 7a. It is hard for the VI learning to recognize and write Braille themselves. Therefore, we developed a Braille recognition system, which consists of a glove based on 2B-sensor, a tailored Braille board and a microprogrammed control unit (MCU) processing unit connected to the computer for receiving and analyzing data (Figure 7a, b). The Braille recognition system transmits the Braille touching signals to acoustic signals through a process circuit and a MCU. As shown in Figure 7c and Movie S1, during the Braille learning process, the VI touch and learn the Braille at first, then write the Braille. The Braille recognition system can be used to check the written Braille through transforming the tactile signals to acoustic signals high-efficiently. Therefore, the developed Braille recognition system based on high-accuracy 2B-sensor will be helpful for the VI learning Braille, then reading, writing and communicating with the outside.

CONCLUSIONS

In summary, a Braille recognizing system was fabricated utilizing a tailored micro-dome sensor with a high-efficient AI method. The Braille recognizing system possesses a continuous, stable durable and cost-efficient

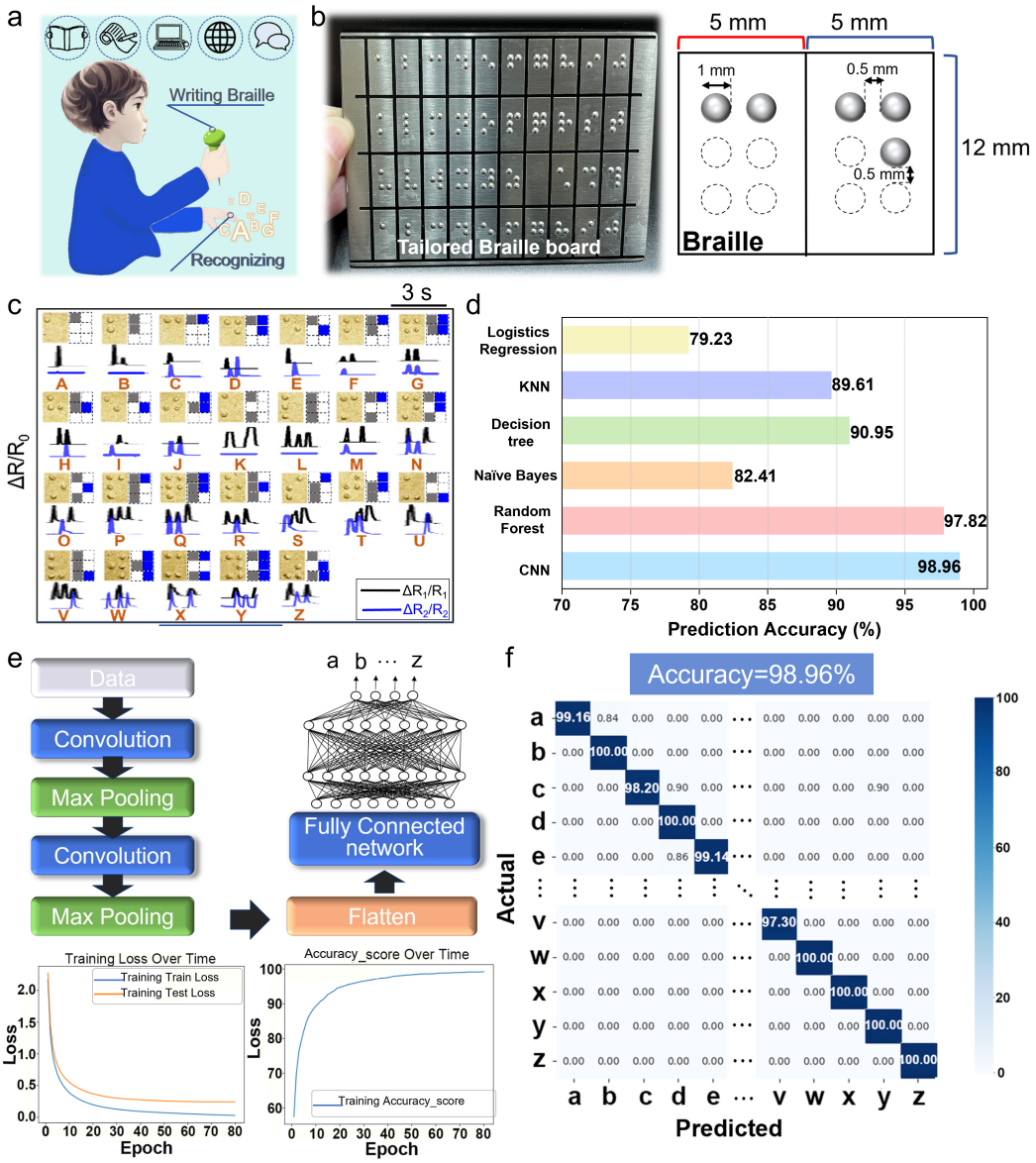

Figure 6 Braille recognizing methods of tactile sensor. (a) Schematic illustration of the Braille learning is crucial for the VI reading, learning and communicating with the world. (b) Photograph of the tailored Braille board for learning Braille by the developed sensors. (c) Digital photo showing a Braille board with twenty-six English letters and relative resistance change response curves when sliding the sensor unit across the Braille board one by one through the 2B-sensor. (d) Evaluation results of Braille recognition based on six kinds of machine learning methods. (e) Processing methods of machine learning. (f) Confusion matrix of twenty-six letters with a two-channel 2B-sensor.

method for AI learning and recognizing Braille. The developed micro-dome tactile sensor interacting with machine learning method, producing stable and accurate sensing signals by sliding over Braille. Then the sensing signals enhances the recognition system's accuracy and also simplifies data processing, making it highly computationally efficient. Currently, the system supports 26 English letters, with a maximum recognition accuracy of 98.96%, which surpasses most of the other intelligent Braille recognition systems. The proposed fabrication strategy will be highly applicable to help the VI perceive and communicate with the world.

Figure 7 Intelligent interaction application scenario. (a) Schematic illustration of writing and touching Braille "Q", and the photograph of the Braille recognition system including 2B-sensor, Braille board, process circuit and MCU. (b) The working process of the Braille recognition system. (c) Applications of the two-channel 2B-glove for learning, writing and recognizing Braille.

MATERIALS AND METHODS

Fabrication of tailored micro-dome tactile sensor

At first, a micro-patterned mold was printed via a two-photon laser direct writing process (Nanoscribe, Germany). Then PDMS prepolymer (Dow Corning, Sylgard 184) was poured into the printing mold, then get rid of gas bubbles in vacuum for 20 min at room temperature, and completely cured at 75 °C for 2 h in the oven. Finally, the micropatterned PDMS film was obtained. The PDMS film was sliced by a laser direct writing machine (Spirit SI-60TI, GCC LaserPro, China). Then, the conductive PDMS films were obtained by nitrogen gas plasma treatment, spraying WPU solution (5%) and magnetron sputtering Ag layer.

Materials characterization

The morphology of the micropatterned sensor was observed via SEM (JEOL JSM-840, Japan). All of the

sensing performances of the flexible micro-patterned sensors were evaluated using a System Source Meter (Model 2601B, Keithley). The spectra were measured using a Nicolet 5700 FTIR spectrometer (Thermo Nicolet Corp, USA). The contact angles of the water droplets were tested by a Contact Angle Analyzer (JY-PHb, China). Droplets of distilled water, with a volume of 3 μL, were placed gently onto the surface at room temperature and pressure.

Data availability

The original data are available from the corresponding authors upon reasonable request.

Funding

This work was supported by the National Natural Science Foundation of China (62201537), the Natural Science Foundation of Shandong Province (ZR2022QF008), the Shandong Province Science and Technology SMES Innovation Ability Improvement Project (2024TSGC1015), the Qingdao Key Technology Breakthrough Project for Industrial Cultivation and Leadership (International and HongKong Science and Technology Cooperation) (25-1-1-gjgg-96-hz), the Joint Key Innovation Project of the Yangtze River Delta Science and Technology Innovation Community (2023CSJZN0203), and the China Postdoctoral Science Foundation (2025M770666).

Author contributions

L.W. was responsible for methodology, investigation, resources, writing original draft, writing review & editing; Z.Z. was responsible for investigation, software and writing original draft; X.A. was responsible for software and investigation; J.L. was responsible for methodology and data curation; L.Q. was responsible for resources. J.L. was responsible for writing review & editing and funding acquisition; M.T. was responsible for resources, methodology, writing review & editing; Q.W. was responsible for investigation, validation, resources, and funding acquisition.

Conflict of interest

The authors declare no conflict of interest.

Supplementary information

The supporting information is available online at https://doi.org/10.1360/nso/20250078. The supporting materials are published as submitted, without typesetting or editing. The responsibility for scientific accuracy and content remains entirely with the authors.

References

1 Liu YH, Wang JJ, Wang HZ, *et al.* Braille recognition by E-skin system based on binary memristive neural network. *Sci Rep* 2023; **13**: 5437.

2 Qu X, Ma X, Shi B, *et al.* Refreshable Braille display system based on triboelectric nanogenerator and dielectric elastomer. *Adv Funct Mater* 2021; **31**: 2006612.

3 Liu W, Yu W, Li K, *et al.* Enhancing blind-dumb assistance through a self-powered tactile sensor-based Braille typing system. *Nano Energy* 2023; **116**: 108795.

4 Dai X, Huang LB, Sun Z, *et al.* A phonic Braille recognition system based on a self-powered sensor with self-healing ability, temperature resistance, and stretchability. *Mater Horiz* 2022; **9**: 2603–2612.

5 Tanaka M, Miyata K, Chonan S. A wearable Braille sensor system with a post processing. *IEEE ASME Trans Mechatron* 2007; **12**: 430–438.

6 Nahar L, Sulaiman R, Jaafar A. An interactive math braille learning application to assist blind students in Bangladesh. *Assistive Tech* 2022; **34**: 157–169.

7 Doi K, Nishimura T, Takei M, *et al.* Braille learning materials for Braille reading novices: Experimental determination of dot code printing area for a pen-type interface read aloud function. *Univ Access Inf Soc* 2021; **20**: 45–56.

8 Zhao XF, Hang CZ, Lu HL, *et al.* A skin-like sensor for intelligent Braille recognition. *Nano Energy* 2020; **68**: 104346.

9 Ling Y, Gong S, Zhai Q, *et al.* Embedding pinhole vertical gold nanowire electronic skins for Braille recognition. *Small* 2019; **15**: 1804853.

10 Niu H, Li H, Li Y, *et al.* Cocklebur-inspired "branch-seed-spininess" 3D hierarchical structure bionic electronic skin for intelligent perception. *Nano Energy* 2023; **107**: 108144.

11 Qiao Y, Jian J, Tang H, *et al.* An intelligent nanomesh-reinforced graphene pressure sensor with an ultra large linear range. *J Mater Chem A* 2022; **10**: 4858–4869.

12 Lai Q, Zhao X, Sun Q, *et al.* Emerging MXene-based flexible tactile sensors for health monitoring and haptic perception. *Small* 2023; **19**: 2300283.

13 Lv C, Tian C, Jiang J, *et al.* Ultrasensitive linear capacitive pressure sensor with wrinkled microstructures for tactile perception. *Adv Sci* 2023; **10**: 2206807.

14 Yuan S, Bai J, Li S, *et al.* A multifunctional and selective ionic flexible sensor with high environmental suitability for tactile perception. *Adv Funct Mater* 2024; **34**: 2309626.

15 Davoodi E, Montazerian H, Haghniaz R, *et al.* 3D-printed ultra-robust surface-doped porous silicone sensors for wearable biomonitoring. *ACS Nano* 2020; **14**: 1520–1532.

16 Sang Z, Ke K, Manas-Zloczower I. Design strategy for porous composites aimed at pressure sensor application. *Small* 2019; **15**: 1903487.

17 Yang R, Dutta A, Li B, *et al.* Iontronic pressure sensor with high sensitivity over ultra-broad linear range enabled by laser-induced gradient micro-pyramids. *Nat Commun* 2023; **14**: 2907.

18 Tao K, Chen Z, Yu J, *et al.* Ultra-sensitive, deformable, and transparent triboelectric tactile sensor based on micro-pyramid patterned ionic hydrogel for interactive human-machine interfaces. *Adv Sci* 2022; **9**: 2104168.

19 Zhang C, Liu S, Huang X, *et al.* A stretchable dual-mode sensor array for multifunctional robotic electronic skin. *Nano Energy* 2019; **62**: 164–170.

20 Mao Y, Ji B, Chen G, *et al.* Robust and wearable pressure sensor assembled from AgNW-coated PDMS micropillar sheets with high sensitivity and wide detection range. *ACS Appl Nano Mater* 2019; **2**: 3196–3205.

21 Wang L, Liu J, Qi X, *et al.* Personal protective gloves with objects recognizing for rescuing in disaster. *Chem Eng J* 2023; **477**: 146986.

22 Ji B, Zhou Q, Lei M, *et al.* Gradient architecture-enabled capacitive tactile sensor with high sensitivity and ultrabroad linearity range. *Small* 2021; **17**: 2103312.

23 Fuh YK, Wang BS, Tsai CY. Self-powered pressure sensor with fully encapsulated 3D printed wavy substrate and highly-aligned piezoelectric fibers array. *Sci Rep* 2017; **7**: 6759.

24 Lin C, Lan J, Yu J, *et al.* Cocklebur-structured design of plant fibers for high-performance triboelectric nanogenerators and pressure sensors. *Mater Today Commun* 2022; **30**: 103208.

25 Bai X, Gai C, Wu D, *et al.* Intelligent sensing system of the car seat with flexible piezoresistive sensor of double-layer conductive network. *IEEE Sens J* 2022; **22**: 3113–3121.

26 Chen B, Zhang L, Li H, *et al.* Skin-inspired flexible and high-performance MXene@polydimethylsiloxane piezoresistive pressure sensor for human motion detection. *J Colloid Interface Sci* 2022; **617**: 478–488.

27 Li S, Liu G, Wen H, *et al.* A skin-like pressure- and vibration-sensitive tactile sensor based on polyacrylamide/silk fibroin elastomer. *Adv Funct Mater* 2022; **32**: 2111747.

28 Kurup LA, Cole CM, Arthur JN, *et al.* Graphene porous foams for capacitive pressure sensing. *ACS Appl Nano Mater* 2022; **5**: 2973–2983.

29 Fu X, Li J, Li D, *et al.* MXene/ZIF-67/PAN nanofiber film for ultra-sensitive pressure sensors. *ACS Appl Mater*

Interfaces 2022; **14**: 12367–12374.

30 Zheng Q, Lee J, Shen X, *et al.* Graphene-based wearable piezoresistive physical sensors. *Mater Today* 2020; **36**: 158–179.

31 Shokat S, Riaz R, Rizvi SS, *et al.* Characterization of English Braille patterns using automated tools and RICA based feature extraction methods. *Sensors* 2022; **22**: 1836.

32 Bhatia S, Devi A, Alsuwailem RI, *et al.* Convolutional neural network based real time arabic speech recognition to arabic Braille for hearing and visually impaired. *Front Public Health* 2022; **10**: 898355.

33 Kausar T, Manzoor S, Kausar A, *et al.* Deep learning strategy for Braille character recognition. *IEEE Access* 2021; **9**: 169357–169371.

34 Gao Z, Chang L, Ren B, *et al.* Enhanced braille recognition based on piezoresistive and piezoelectric dual-mode tactile sensors. *Sens Actuat A-Phys* 2024; **366**: 115000.

35 Lu Y, Kong D, Yang G, *et al.* Machine learning-enabled tactile sensor design for dynamic touch decoding. *Adv Sci* 2023; **10**: 2303949.

36 Hsu BM. Braille recognition for reducing asymmetric communication between the blind and non-blind. *Symmetry* 2020; **12**: 1069.

37 Tabassum R, Ashfaq M, Oku H. Development of an efficient, one-pot, multicomponent protocol for synthesis of 8-hydroxy-4-phenyl-1,2-dihydroquinoline derivatives. *J Heterocyclic Chem* 2021; **58**: 534–547.